Comparison of Global and Local Array Topologies for SENSE Imaging

D. K. Spence[1], S. M. Wright[1]

[1]Texas A&M University, College Station, TX, United States

Introduction

In an effort to improve arrays for SENSE imaging, different array topologies need to be examined and compared. The two prerequisites for a good array are high intrinsic signal to noise ratio (SNR) and low noise amplification (g-factor) during reduced image acquisitions. In this abstract, the merits of two classes of planar arrays are discussed; arrays composed of small elements with "local" sensitivity versus arrays made up of elements that have a "global" sensitivity over the entire FOV.

Methods

Two arrays, each having four elements, were examined. The first is a linear array composed of four loops (Fig 1a). The second is a stacked array made of four global elements (Fig 1b). Both arrays had overall dimensions of 5cm by 5cm and were positioned in the coronal plane. In the linear array, the loops are overlapped to reduce nearest neighbor coupling. In the stacked array, the elements are symmetric about the center of the array. Ideally, this symmetry will inherently decouple the array elements.

Initially, the designs were modelled in Matlab®. The magnetic field senstivities and magnetic vector potentials of the array elements were computed using the quasi-static approximation. The mutual resistance matrix for the array was computed from the sample losses. Radiation and conductor losses were not included in the model. In general, the maximum combined SNR of an array for a given point in the image may be calculated as $SNR_{\max} = \sqrt{\mathbf{B}^T \Psi^{-1} \mathbf{B}}$ where $\mathbf{B}$ is the vector containing the coil sensitivities at the given point, and Ψ is the noise correlation matrix for the array(1,2). In SENSE imaging, the maximum SNR at a pixel is dependent upon the reduction factor, R, and the geometry factor, g (3). The geometry factor is defined as $g_{(x,y)} = \sqrt{\left(\mathbf{S}^T \Psi^{-1} \mathbf{S}\right)^{-1}_{(x,y),(x,y)} \cdot \left(\mathbf{S}^T \Psi^{-1} \mathbf{S}\right)_{(x,y),(x,y)}}$, where $\mathbf{S}$ is a matrix containing the coil sensitivities at the aliased pixels. The maximum combined SNR for a pixel in a SENSE image is then $SNR_{\max} = \sqrt{\mathbf{B}^T \Psi^{-1} \mathbf{B}} \big/ g\sqrt{R}$.

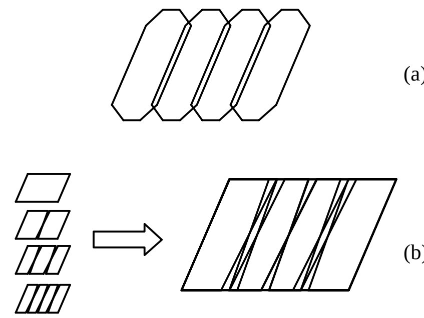

Figure 1. Topologies of the four element local array (a) and the four element global array (b).

Results

SNR curves along the major axes were computed and the results are shown in figure 2. The x-axis and z-axis curves were computed in a plane 1.5 centimeters above the array surface. The y-axis curve passes through the origin. In general, the global array shows better SNR than the local array. As the imaging plane moves away from the array surface, the SNR values of the two arrays converge. Along the z-axis of the coronal plane, the global array has nearly twice the SNR and greater homogeneity. However, along the x-axis of the same plane, the local array exhibits greater homogeneity though its SNR is still approximately half that of the global array. The global array SNR also falls off more rapidly along the z-axis and eventually becomes less than the local array SNR. Figure 3 shows the g-factor maps for the arrays corresponding to an image FOV of 2.5cm by 2.5cm in the coronal plane and reduction factors of two, three, and four.

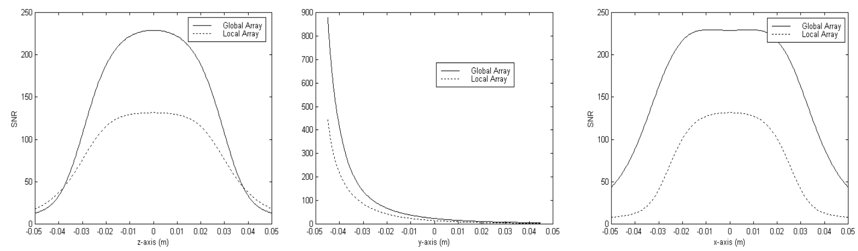

Figure 2. SNR curves along the x, y, and z axes.

Discussion

Surprisingly, despite the arrays having very different topologies, the g-factor plots were quite similar. At a reduction factor of two, the arrays performed almost identically in terms of g-factor. At higher reduction factors, the local array clearly performed better given this image FOV. In terms of overall SNR, the global array proves to be superior, particularly in regions near the array surface. Since a higher SNR mitigates the effects of a poor g-factor, the global array appears to be superior.

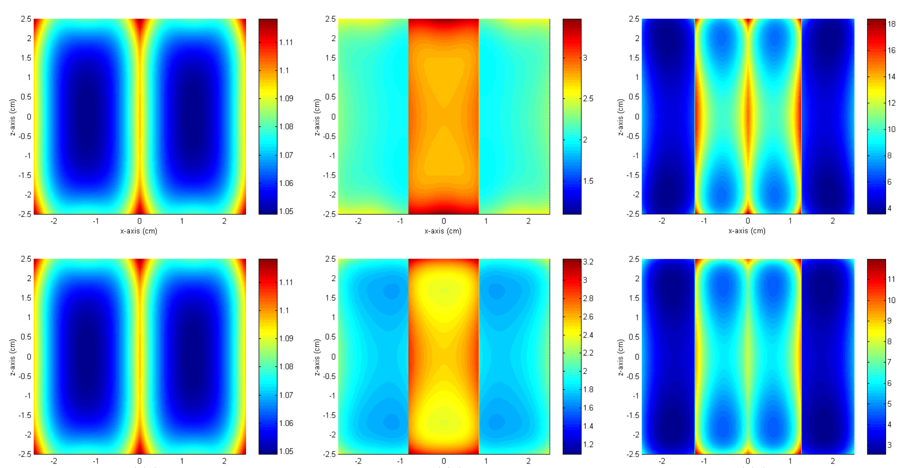

Figure 3. G-factor maps of the global array, top row, and the local array, bottom row, for reduction factors of two, three, and four.

References

1. Wang J, Reykowski A, Dickas J. IEEE Trans Biomed Eng 1995;42(9):908-917.
2. Roemer PB, Edelstein WA, Hayes CE, Souza SP, Mueller OM. Magn Reson Med 1990;16(2):192-225.
3. Pruessmann KP, Weiger M, Scheidegger MB, Boesiger P. Magn Reson Med 1999;42(5):952-962.
4. H. Fujita, DK Spence. Proceedings 2000 ISMRM, Hawaii.